*Metals* **2014**, *4*, 108-117; doi:10.3390/met4020108

OPEN ACCESS

*metals*

**ISSN 2075-4701**

www.mdpi.com/journal/metals/

*Article*

# Surface Growth and Diffusion Energetics of Ag Monolayers on Cu (001)

**Georgios S.E. Antipas**

School of Mining Engineering and Metallurgy, National Technical University of Athens, Zografou Campus, Athens 15780, Greece; E-Mail: gantipas@metal.ntua.gr; Tel.: +30-210-7722037; Fax: +30-210-7722168

*Received: 9 February 2014; in revised form: 14 March 2014 / Accepted: 26 March 2014 / Published: 4 April 2014*

**Abstract:** The growth of Ag monolayers on Cu (001) was studied by periodic Density Functional Theory (DFT). Despite the limited solid solubility of Ag in Cu, the growth of a single Ag overlayer on Cu (001) was predicted as feasible. In contrast, the growth of consecutive Ag monolayers was found to be energetically forbidden. Inter-diffusion of Ag monolayers into Cu was raised as a possibility but it was dependent on the sequence in which the Ag monolayers were introduced into the Cu bulk. The Ag layers preferred to be kept neither too far apart nor too close to each other, the optimum spacing between two Ag monolayers determined to be that of two consecutive Cu layers. Ag diffusion mediated tensile stress in the Cu cell by causing an increase of the unit cell constant by as much as 22%. Interactions between the Ag and Cu species also involved a degree of covalency. In general, progression of a surface Ag monolayer into the Cu bulk involved charge depletion over the Ag species and a simultaneous charge concentration over neighboring Cu atoms; this mechanism was found to influence Cu up to a depth of four surface layers.

**Keywords:** Ag monolayers; Cu (001); surface alloying; surface growth; diffusion; *ab initio* energetics; epitaxial growth

## 1. Introduction

Interface phenomena occurring between metallic monolayers become of interest in cases where end-product mechanical properties depend on structural discontinuity across the interface [1]. These phenomena are particularly relevant to nanofabrication techniques, such as scanning-probe techniques,

self-assembly (including epitaxial methods) [2], strain engineering [3], e-beam nanofabrication [4] and template manufacturing [5]. Continuous improvements in nanofabrication processing over the period of the last two decades have stimulated demand for next-generation computation and communication devices. A characteristic example of potential advancement for computation lies in the fabrication of nm-sized transistors with a resolution beyond 32 nm [6]. The fundamental interest in the submicron range stems from the potential to access and manipulate electrical [7], magnetic, optical, thermal and mechanical properties such as conductance quantization [8], bandgap modification [9] and coulomb blockade [10]. All of these properties arise from confinement of charged carriers, in structures such as quantum wells, wires and dots and the successful manipulation of these properties stimulates promise for novel devices. This is because nm-sized devices dimensions exhibit improved characteristics compared to larger devices; typical examples of such improvements in the case of quantum dot lasers are lower threshold currents [11], augmented dynamic responses and enhanced emission line widths [12].

On the materials engineering front, interface phenomena may become important even in cases of complete elemental immiscibility, leading to layered structures under certain conditions. For example, the stability and mechanical properties of TM/Cu systems are governed by a number of factors, including lattice mismatch, internal stress [13], island formation alloyed surface layers [14], and inter diffusion [15] and are affected by in-plane grain size [16], as is the case of vapor-deposited thin films formed by 3d- and 4d-transition metal layers (typically of Ni [17], Mn [18], Cr [19], V [20], Co [21], and Pt [22]) on a Cu substrate. In fact, the topmost crystal layer has been found to determine the Kondo temperature through a localized interaction of its own d-levels with the d-bands of the bulk [23]. Of the various TM additions, the epitaxial growth and diffusion of Ag layers on Cu is particularly intriguing. Auger spectroscopy has shown that the energy position of the d band shifts from about 4 eV to 3 eV below the Fermi level upon formation of an Ag monolayer on Cu; this effect has been attributed to a static electron transfer between the Ag and Cu atoms, but this interpretation is seemingly in contradiction with the similarity in electronegativity between the Ag and Cu atoms. Ag-adlayer 4d states, measured in the surface Brillouin zone center, have shown substrate-dependent shifts [24]. In fact, the charge perturbation brought about by the epitaxial growth of a single Ag monolayer on Cu (111) has been reported to extend down to as much as ten bulk atomic layers [25]. This finding is on a par with LEEDS studies of the coadsorption of dissimilar metal atoms on fcc metal substrates which have demonstrated the formation of ordered mixed surface structures, in which considerable restructuring of the substrate surface atoms occurred [26]. The restructuring mediated an indirect, cooperative interaction between coadsorbates through the substrate surface [26], supplementary to a stabilizing, direct interaction between coadsorbates.

The current work was motivated by the facility to create three-dimensional quantum confinement structures by restricting epitaxial growth of a quantum-well material to nanometer-scale regions (e.g., [27]) and reports on the possibility of surface growth, inter-diffusion, and alloying of Ag (001) monolayers on Cu (001) from the standpoint of DFT total formation energy.

## 2. Results and Discussion

Formation energies normalized by the number of electrons and Fermi energy limits as calculated by DFT are listed in Table 1, both for relaxed and non relaxed cluster geometries. The lattice spacing of

the relaxed Cu slab at the BLYP/TZ2P level was equal to 3.619 Å, in agreement with the experimental value [28]. In all cases, the isolated Cu slab was found to be energetically more stable than any of its combinations with Ag adlayers, a feature which stems from low Ag-Cu solubility.

**Table 1.** Formation energies for surface alloying, surface growth and inter-diffusion of Ag monolayers on Cu (001).

| Cluster designation | Formation energy (ma.u.) non relaxed | Formation energy (ma.u.) relaxed | Fermi energy (a.u.) non relaxed | Fermi energy (a.u.) relaxed |
|---|---|---|---|---|
| Cu4 | −3.152 | −3.152 | −0.2221 | −0.2208 |
| Inter-diffusion | | | | |
| Ag-Cu4 | −2.435 | −2.292 | −0.2227 | −0.2103 |
| Cu-Ag-Cu3 | −2.242 | −2.233 | −0.1949 | −0.1954 |
| Cu2-Ag-Cu2 | −2.225 | −2.466 | −0.2328 | −0.5269 |
| Ag2-Cu4 | 1.221 | 399.518 | −0.2882 | −0.4950 |
| Cu-Ag2-Cu3 | 18.392 | −1.619 | −1.1044 | −0.1788 |
| Cu2-Ag2-Cu2 | −1.632 | −1.629 | −0.1412 | −0.1430 |
| Ag2-Cu4 | 1.221 | 399.518 | −0.2882 | −0.4950 |
| Ag-Cu-Ag-Cu3 | −1.350 | 141.017 | −0.2080 | −0.5484 |
| Ag-Cu2-Ag-Cu2 | 8.089 | −1.011 | −0.4776 | −0.1571 |
| Ag-Cu3-Ag-Cu | −1.888 | 2.455 | −0.2058 | −0.3468 |
| Surface growth | | | | |
| Cu4 | −3.152 | −3.152 | −0.2221 | −0.2208 |
| Ag-Cu4 | −2.435 | −2.292 | −0.2227 | −0.2103 |
| Ag2-Cu4 | 1.221 | 399.518 | −0.2882 | −0.4950 |
| Surface alloying | | | | |
| Ag2-Cu4 | 1.221 | 399.518 | −0.2882 | −0.4950 |
| Ag-Cu-Ag-Cu3 | −1.350 | 141.017 | −0.2080 | −0.5484 |
| Cu-Ag-Cu2-Ag-Cu | −1.736 | −2.044 | −0.2230 | −0.2071 |
| Ag-Cu2-Ag-Cu2 | 8.089 | −1.011 | −0.4776 | −0.1571 |

### *2.1. Surface Growth of Ag Monolayers*

Results indicated that surface stability of a single Ag monolayer is a possibility, albeit at formation energy roughly 20% lower to that of the bulk Cu slab (see Figure 1a and data in Table 1).Perhaps counter-intuitively, addition of a second surface Ag monolayer was found to be energetically infeasible due to the dissociation of the outer Ag monolayer (see Figure 1b). Voronoi deformation density (VDD) analysis revealed that the preference towards a single Ag monolayer was due to charge transfer, as shown in Figure 2: Initial formation of the monolayer on the Cu slab surface was accompanied by a pronounced charge concentration over Cu surface atoms, at approximately tenfold the density of the isolated Cu slab; this was accompanied by charge depletion from the Ag monolayer atoms, which effectively introduced an electrostatic cohesive effect in the Ag/Cu interface. Additionally, some Ag/Cu covalency was also present, as indicated by the overlap of valence $t_{1u}$ populations at approximately −0.380 a.u. (see pDOS curves in Figure 1a). This observation is in agreement with Auger spectroscopy results for the case of Ag epitaxial growth on Cu (111) [29]. The possibility of a Ag monolayer has also been raised by Christensen *et al.* [30] and has been established experimentally

by Sprunger *et al.* [31]; the latter work reported that alloying may indeed occur for small concentrations of Ag deposited on Cu (100). Moreover, a previous DFT study of the growth of an Ag monolayer on Cu (110) has indicated extended matching of the electron wavefunctions at the interface [24].

**Figure 1.** Density of stated (DOS) of the two cluster models for surface growth. The Fermi energy is marked by a vertical line. Atom notation: White—Ag, bronze—Cu. (**a**) Ag-d (thick black line) and Cu-d states (thin grey line). Also shown are Voronoi deformation density (VDD) values of the top four surface layers of the Cu slab surrounded by an iso-density surface of 0.04 a.u. Notation is followed throughout; (**b**) Addition of a second Ag monolayer and corresponding DOS and VDD values.

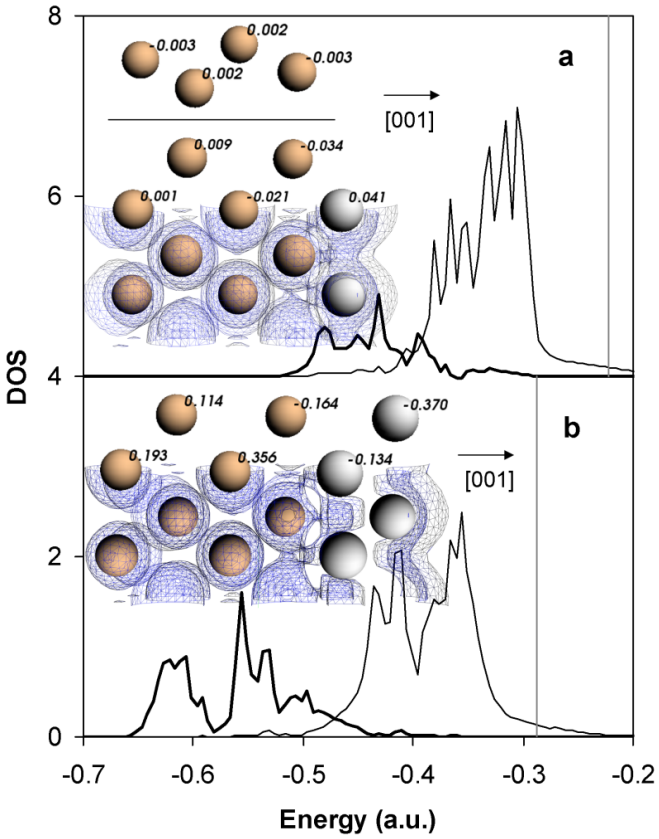


Upon deposition of the second Ag monolayer (see Figure 1b), charge was depleted from the lower Cu layers and was distributed over the surface Cu layer as well as over both Ag monolayers. This resulted in electrostatic repulsion between the two Ag layers and the Cu slab and a further disruption of cohesive charge density, as shown by the iso-density surfaces in Figure 1b. Most importantly, however, addition of the second Ag monolayer resulted in the breakdown of covalent binding, between both Ag layers and the Cu slab (see pDOS lack of Ag/Cu $t_{1u}$ populations in Figure 1b).It was, thus, concluded that while surface growth of a single Ag monolayer is feasible, growth of consecutive monolayers is not a possibility. It has to be noted that this finding is in some contrast with the experimentally observed growth of up to four atomic layers of Ag (111) on Cu (111) [27].

Stability of an Ag monolayer deposited on Cu (001) was considered next, where deposition may be followed by inter-diffusion (absorption of the monolayer in the bulk Cu layers).

**Figure 2.** Alloying/inter-diffusion sequence. Numbers between atoms (in black font) denote relaxed geometry interatomic spacings in Å. Numbers in purple font are Voronoi deformation charges (a.u.) for the non relaxed (top number) and relaxed (bottom number) geometries. All un-relaxed interatomic spacings (not shown) are equal to 3.615 Å. All views are along the [0$\bar{1}$0] direction. All iso-density surfaces are drawn at 0.04 a.u.

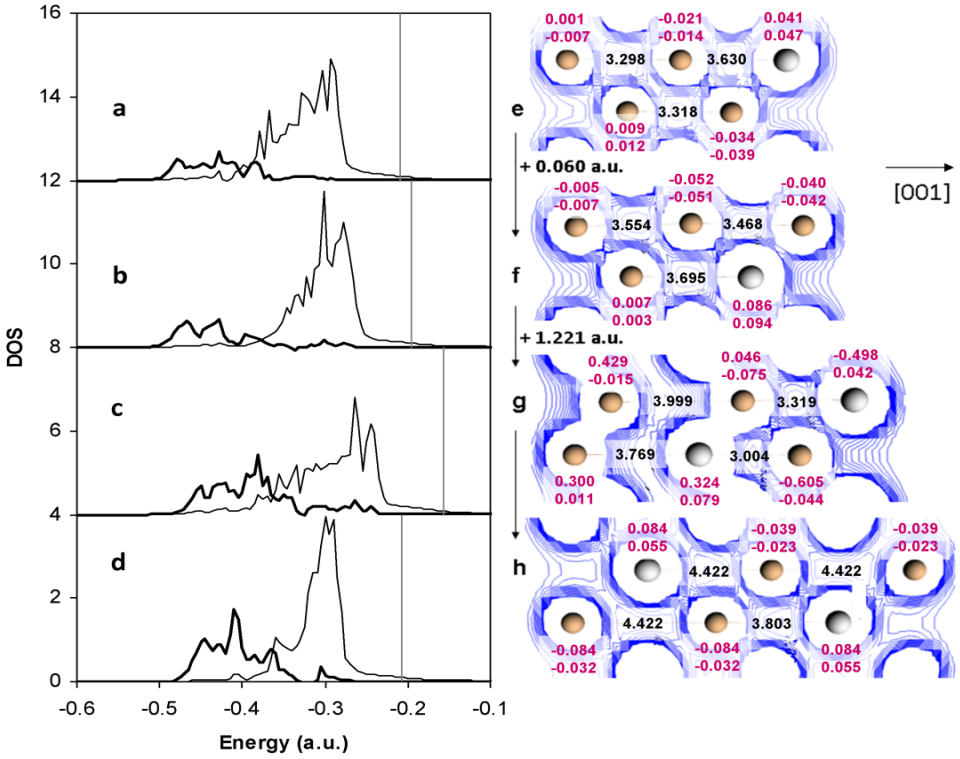


*2.2. Ag Diffusion towards the Cu Bulk*

Diffusion of the Ag monolayer into the Cu bulk was found to be endothermic, by 0.060 a.u. in the BLYP/TZ2P level of theory (see transition from Figure 2e,f). The fundamental reason for the difficulty in inter-diffusion is the absence of covalent interactions, as depicted by the transition from Figure 2a,b, where diffusion into the bulk is accompanied by the absence of Ag-$t_{1u}$ overlap with Cu valence populations. Upon diffusion of the Ag layer into the bulk (see Figure 2f), compressive stress was induced on the upper two Cu overlayers while the rest of the Cu bulk remained under the effect of tensile stress. The compressive stress induced on the outer two Cu layers appeared to be due to increased electrostatic attraction mediated by charge transfer from Ag (see charge depletion shown by the VDD values in Figure 2f) into neighboring Cu atoms. The tensile stress induced to the rest of the Cu bulk was due to further charge transferred from the third Cu layer towards closest Cu neighbors. This effect was reproduced by DFT for both the relaxed and the non relaxed geometries.

Further Ag diffusion into the Cu bulk was increasingly endothermic (see transition from Figure 2f,g and associated DOS in Figure 2b,c, respectively).The diffusing Ag layer as well as the Cu layer immediately below it (*i.e.*, the fourth Cu surface layer) were further depleted of charge which was concentrated over nearest Cu neighbors (see Figure 2g). In the same cluster, DFT results indicated that surface growth of an additional Ag monolayer restored covalent interaction of the Ag and Cu d states (e.g., see orbital states at −0.35 a.u. in Figure 2c) and also promoted further diffusion of the Ag

monolayers (see Figure 2h) as well as further mixing between d states (see Figure 2c).This finding is on par with previous angle-resolved photoemission studies of the growth of Ag (111) on various substrates [32]. Further progression of the Ag overlayer into the Cu bulk proceeded spontaneously (see Figure 2h), again accompanied by charge transfer from Ag into closest Cu neighbors and firm covalent interactions between the species' d states at around −0.3 a.u. (see Figure 2d).Also, the unit cell was under a tensile stress along [100], as revealed by the 22% increase in the lattice constant. Interestingly, the lower Ag layer and its surrounding Cu atoms experienced charge concentration, which suggested charge depletion around Cu atoms deeper in the cluster.

Figure 3 presents a view of alloying and inter-diffusion from the perspective of VDD for each of the atomic layers involved. As may be seen, diffusion of the Ag surface layer into the bulk was always accompanied by charge depletion from Ag, while the charge of the first Cu layer remained largely unaffected. However, the rest of the Cu layers accommodated Ag diffusion in a varied manner: they were all acceptors of charge density, up to the point of diffusion of the second Ag layer into the bulk. After that point, all Cu atoms appear as charge acceptors. To generalize, regardless of the possibility the Cu-Ag-Cu2-Ag-Cu complex formation (Figure 2h), an overlayer of Ag may not be alloyed into bulk Cu, as revealed by the energetics of the Ag-Cu-Ag-Cu3 and Ag-Cu2-Ag-Cu2 complexes (see Table 1). It appears that both consecutive, as well as highly separated Ag layers are forbidding of a stable equilibrium with the Cu substrate. Also, in the case of interface layers, the magnitude of the total energy differences indicates that formation of interlaced Ag and Cu structures is possible at the Ag/Cu interface for low slab thicknesses. Such a result is on a par with experimental atom-probe measurements carried out on thin-layer interfaces of drawn *in situ* composites which were deformed at very high strain, showing intermixing of Ag/Cu [33] and Nb/Cu [34] layers. Overall, the results were not influenced by DFT relaxation.

**Figure 3.** Voronoi deformation density map of all layers for all alloying clusters considered. Each VDD set of points in the graph corresponds to the cluster formation immediately underneath.

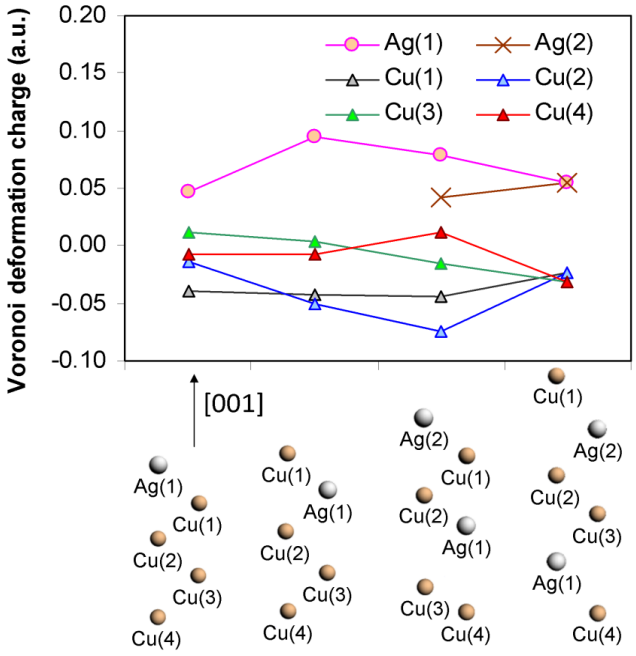

## 3. Materials and Methods

Gas phase, spin unrestricted DFT calculations were performed with the periodic version of the Amsterdam density functional (ADF) program [35,36] within the realm of the generalized gradient approximation (GGA). Electron exchange and correlation were addressed by the BLYP [37,38] functional. Single-electron wavefunctions were expanded using TZ2P uncontracted Slater-type orbitals for all atoms (TZ2P is a triple-ζ basis set with two sets of polarization functions). Core electrons were frozen inclusive of 4p for Ag and 3p for Cu. A 0.1 orbital mixing ratio was kept per SCF step. Our preliminary DFT trials on the system indicated that the most pronounced problem affecting SCF convergence was that of low-lying unoccupied states. To alleviate this, unoccupied level shifts in the range of 0.5 to 2.0 a.u. were used. Additionally, the calculations were corrected for relativistic effects using the zero-order regular approximation (ZORA) [39].

Cu slabs were created in silico by slicing a number of atomic layers off bulk fcc-Cu along the [001] direction. All slabs were of infinite length and width. The fcc-Cu lattice constant was set to the experimentally observed value of 3.615 Å [28]. A free surface view along the [001] direction of a 10 atomic layer Cu slab is shown in Figure 1a, in which the unit cell is highlighted. fcc-Ag monolayers along the [001] direction were produced by the same method; a typical Ag (001) monolayer is shown in Figure 1b; the fcc-Ag lattice constant was set to the experimentally established value of 4.0853 Å. Ag atoms were introduced to the Cu slab by substitution of surface Cu atoms. Figure 2 shows a [001] view of such a super cell in which a unit cell is highlighted. The original structures were used as starting geometries for relaxation DFT, followed by single point and frequency calculations to confirm convergence via the absence of imaginary frequencies.

## 4. Conclusions

Surface stability of a single Ag monolayer was found possible at formation energy roughly 20% higher to that of bulk Cu. of a second surface Ag monolayer was found to be energetically infeasible due to dissociative charge transfer as revealed by VDD, which resulted in electrostatic repulsion between the two Ag layers and the Cu slab.

Initial diffusion of a single Ag monolayer into the Cu bulk was found to be endothermic. Further progression of the Ag layer into the Cu bulk was also endothermic, while surface growth of an additional Ag monolayer mediated stabilizing covalent interaction of the Ag and Cu d states.

Progression of the two Ag layers further into the bulk could proceeded spontaneously, accompanied by charge depletion from Ag into closest Cu neighbors and enhanced covalent interaction between the species' d states.

Ag inter-diffusion induced a tensile stress in the unit cell.

## Conflicts of Interest

The author declares no conflict of interest.

## References


1. Misra, A.; Verdier, M.; Lu, Y.C.; Kung, H.; Mitchell, T.E.; Nastasi, M.; Embury, J.D. Structure and mechanical properties of Cu-X (X = Nb, Cr, Ni) nanolayered composites. *Scr. Mater.* **1998**, *39*, 555–560.
2. Bimberg, D.; Grundmann, M.; Ledentsov, N.N. *Quantum Dot Heterostructures*; John Wiley: Chichester, UK, 1999; Volume 471973882.
3. Herman, M.A.; Sitter, H. *Molecular Beam Epitaxy: Fundamentals and Current Status*; Springer-Verlag: Berlin, Germany, 1989.
4. Rai-Choudhury, P. *Handbook of Microlithography, Micromachining and Microfabrication: Microlithography*; IET SPIE Press: Bellingham, WA, USA, 1997; Volume 1.
5. Whitesides, G.M.; Grzybowski, B. Self-assembly at all scales. *Science* **2002**, *295*, 2418–2421.
6. Tarutani, S.; Tsubaki, H.; Kanna, S. Development of materials and processes for double patterning toward 32-nm node 193-nm immersion lithography process. In Proceedings of the SPIE Advanced Lithography, International Society for Optics and Photonics, San Jose, CA, USA, 3 March 2008; doi:10.1117/12.771773.
7. Ruffino, F.; Canino, A.; Grimaldi, M.G.; Giannazzo, F.; Bongiorno, C.; Roccaforte, F.; Raineri, V. Self-organization of gold nanoclusters on hexagonal SiC and $SiO_2$ surfaces. *J. Appl. Phys.* **2007**, *101*, 064306.
8. Terabe, K.; Hasegawa, T.; Nakayama, T.; Aono, M. Quantized conductance atomic switch. *Nature* **2005**, *433*, 47–50.
9. Okazaki, T.; Okubo, S.; Nakanishi, T.; Joung, S.-K.; Saito, T.; Otani, M.; Okada, S.; Bandow, S.; Iijima, S. Optical band gap modification of single-walled carbon nanotubes by encapsulated fullerenes. *J. Am. Chem. Soc.* **2008**, *130*, 4122–4128.
10. Park, J.; Pasupathy, A.N.; Goldsmith, J.I.; Chang, C.; Yaish, Y.; Petta, J.R.; Rinkoski, M.; Sethna, J.P.; Abruña, H.D.; McEuen, P.L. Coulomb blockade and the Kondo effect in single-atom transistors. *Nature* **2002**, *417*, 722–725.
11. Adachi, M.; Yoshizumi, Y.; Enya, Y.; Kyono, T.; Sumitomo, T.; Tokuyama, S.; Takagi, S.; Sumiyoshi, K.; Saga, N.; Ikegami, T. Low threshold current density InGaN based 520–530 nm green laser diodes on semi-polar {2021} free-standing GaN substrates. *Appl. Phys. Express* **2010**, *3*, 121001.
12. Strauf, S.; Hennessy, K.; Rakher, M.; Choi, Y.-S.; Badolato, A.; Andreani, L.; Hu, E.; Petroff, P.; Bouwmeester, D. Self-tuned quantum dot gain in photonic crystal lasers. *Phys. Rev. Lett.* **2006**, *96*, 127404.
13. Kim, S.H.; Lee, K.S.; Min, H.G.; Seo, J.; Hong, S.C.; Rho, T.H.; Kim, J.S. Surface growth of Ni atoms deposited on a Cu(001) surface. *Phys. Rev. B* **1997**, *55*, 7904–7909.
14. Yang, Z.; Gavrilenko, V.I.; Wu, R. First-principle study of the atomic structure and magnetic properties of ultrathin Ni films on Cu (001) substrate. *Surf. Sci.* **2000**, *447*, 212–218.
15. D'Addato, S.; Finetti, P. Extended X-ray absorption fine structure study of Mn ultrathin films grown on Cu (100). *Surf. Sci.* **2001**, *471*, 203–208.
16. Mašek, K.; Matolín, V. RHEED study of Nb thin film growth on Cu (111) and (100) single-crystals.*Vacuum* **2001**, *61*, 217–221.

17. Asada, T.; Blügel, S. Total energy spectra of complete sets of magnetic states for fcc-Fe films on Cu (100). *Phys. Rev. Lett.* **1997**, *79*, 507–510.
18. Eder, M.; Hafner, J.; Moroni, E.G. Structure and magnetic properties of thin Mn/Cu (001) and CuMn/Cu (100) films. *Surf. Sci.* **1999**, *423*, L244–L249.
19. Adachi, K.; Tsubokawa, S.; Takeuchi, T.; Suzuki, H.G. Strengthening mechanism of cold-drawn wire of *in situ* Cu-Cr composite. *Nippon Kinzoku Gakkaishi/J. Jpn. Inst. Met.* **1997**, *61*, 397–403.
20. Kang, B.S.; Chung, J.S.; Oh, S.K.; Kang, H.J. Energetics of 3d thin film on Cu (001): CuNi surface alloy. *J. Magn. Magn. Mater.* **2002**, *241*, 415–421.
21. Yang, Z.; Wu, R. Intermixing at Nin/Cu (001) interface and its effects on the magnetic properties of Ni. *Surf. Sci.* **2002**, *496*, L23–L28.
22. Blum, V.; Rath, C.; Müller, S.; Hammer, L.; Heinz, K.; García, J.M.; Ortega, J.E.; Prieto, J.E.; Hernán, O.S.; Gallego, J.M.;*et al.* Fe thin-film growth on Au(100): A self-surfactant effect and its limitations. *Phys. Rev. B* **1999**, *59*, 15966–15974.
23. Schneider, M.A.; Wahl, P.; Diekhöner, L.; Vitali, L.; Wittich, G.; Kern, K. Kondo effect of Co adatoms on Ag monolayers on noble metal surfaces. *Jpn. J. Appl. Phys.* **2005**, *44*, 5328–5331.
24. Pletikosić, I.; Mikšić Trontl, V.; Milun, M.; Šokčević, D.; Brako, R.; Pervan, P. D-band quantum well states in Ag(111) monolayer films; substrate-induced shifts. *J. Phys.* **2008**, *20*, 355004.
25. Mottet, C.; Tréglia, G.; Legrand, B. Topology of a Ag monolayer on a Cu (111) substrate: A tight-binding quenched molecular dynamics study. *Surf. Sci.* **1993**, *287–288*, 476–481.
26. Tochihara, H.; Chen, M.-S.; Shirasawa, T.; Mizuno, S. Ordered mixed surface structures formed by coadsorption of dissimilar metal atoms on Cu (001). *Vacuum* **2004**, *74*, 121–131.
27. York, S.M.; Jenkins, C.R.; Silva, S.L.; Leibsle, F.M. Ag growth on *N*-modified Cu (111) surfaces: Potential three-dimensional quantum confinement structures. *Surf. Sci.* **2000**, *464*, L752–L758.
28. McMahon, W.E.; Hirschorn, E.S.; Chiang, T.C. Scanning tunneling microscopy study of a Ag monolayer on Cu (111). *Surf. Sci.* **1992**, *279*, L231–L235.
29. Borensztein, Y. Electronic properties of Ag monolayerson (111) Cu. *Europhys. Lett.* **1987**, *4*, 723–728.
30. Christensen, A.; Ruban, A.V.; Stoltze, P.; Jacobsen, K.W.; Skriver, H.L.; Nørskov, J.K.; Besenbacher, F. Phase diagrams for surface alloys. *Phys. Rev. B* **1997**, *56*, 5822–5834.
31. Sprunger, P.T.; Lægsgaard, E.; Besenbacher, F. Growth of Ag on Cu (100) studied by STM: From surface alloying to Ag superstructures. *Phys. Rev. B* **1996**, *54*, 8163–8171.
32. Shapiro, A.P.; Wachs, A.L.; Hsieh, T.C.; Miller, T.; John, P.; Chiang, T.C. Photoemission study of Ag monolayer systems: Effects of the substrate. *Phys. Rev. B* **1986**, *34*, 7425–7428.
33. Ohsaki, S.; Yamazaki, K.; Hono, K. Alloying of immiscible phases in wire-drawn Cu–Ag filamentary composites. *Scr. Mater.* **2003**, *48*, 1569–1574.
34. Sauvage, X.; Thilly, L.; Lecouturier, F.; Guillet, A.; Blavette, D. FIM and 3D atom probe analysis of Cu/Nb nanocomposite wires. *Nanostruct.Mater.* **1999**, *11*, 1031–1039.
35. Baerends, E.J.; Ellis, D.E.; Ros, P. Self-consistent molecular Hartree-Fock-Slater calculations I. The computational procedure. *Chem. Phys.* **1973**, *2*, 41–51.
36. *Amsterdam Density Functional Program*; Theoretical Chemistry, SCM (scm.com); Vrije Universiteit: Amsterdam, The Netherlands, 2012.

37. Becke, A.D. Density-functional exchange-energy approximation with correct asymptotic behavior. *Phys. Rev. A* **1988**, *38*, 3098–3100.
38. Lee, C.; Yang, W.; Parr, R.G. Development of the Colle-Salvetti correlation-energy formula into a functional of the electron density. *Phys. Rev. B* **1988**, *37*, 785–789.
39. Van Lenthe, E.; Baerends, E.J.; Snijders, J.G. Relativistic total energy using regular approximations. *J. Chem. Phys.* **1994**, *101*, 9783–9792.